Int. J. Heat Mass Transfer. Vol. 25, No. 1, pp. 63–75, 1982.
Printed in Great Britain

0017 9310/82/010063 13 $03.00/0
Pergamon Press Ltd.

MATHEMATICAL MODELLING OF BUOYANCY-INDUCED SMOKE FLOW IN ENCLOSURES

N. C. MARKATOS, M. R. MALIN
CHAM Ltd., Bakery House, 40 High St., Wimbledon, London SW19 5AU, U.K.

and

G. COX
Fire Research Station, Borehamwood, Herts, U.K.

(*Received* 3 *February* 1981 *and in revised form* 22 *June* 1981)

Abstract—A computational procedure for predicting velocity and temperature distributions in enclosures containing a fire source is reported. The procedure is based on the solution, in finite-difference form, of the 2-dim. equations for the conservation of mass, momentum, energy, turbulence energy and eddy dissipation rate, with closing expressions for the turbulent viscosity and heat diffusivity. Effects of buoyancy on the turbulence model have been included. The results are shown to be in reasonable agreement with experimental data.

NOMENCLATURE

C_1, C_2, C_3, C_D, constants in the turbulence model;
f, smoke concentration;
g, gravitational acceleration;
G, generation term for turbulent kinetic energy;
$\tilde{h}$, stagnation enthalpy;
k, turbulence kinetic energy;
m_p, mass continuity error at cell P;
p, static pressure;
R_f, flux Richardson number;
S_ϕ, source or sink for the variable ϕ;
T, absolute temperature;
u, v, velocity components in x and y axes;
x, y, Cartesian co-ordinates, x horizontal, y vertical.

Greek symbols

β, coefficient of volumetric expansion;
Γ, exchange coefficient;
σ, Prandtl number;
θ, temperature rise above ambient;
ε, turbulence energy dissipation rate;
ϕ, general dependent variable;
μ, viscosity;
ρ, density.

Subscripts

eff, effective;
t, turbulent;
B, buoyancy;
k, shear;
0, reference value.

1. INTRODUCTION

APART from experience gained from real fires, physical models of fire have been the main source of information guiding the development of fire legislation. In practice this usually means the use of 'scale models', since statistically meaningful studies of 'full-scale' models require prohibitive human and financial resources. The disadvantage of this approach is that complete similarity between full- and scale-models of fire cannot be preserved [1], and a compromise is always reached, relaxing complete scaling rigour for realistic resource allocation. This approach has been termed the 'art of partial modelling' by Spalding [2]. This unsatisfactory situation has long been the only possible approach to deal with the extremely complex phenomena involved. An alternative approach, in principle capable of modelling fire phenomena economically and without the above compromises is to formulate a mathematical model of the system and obtain solutions using numerical procedures over the field of interest. At present, direct solution of the equations of motion, in time-averaged form and with modelled turbulent stresses, lies within reasonable limits of computer usage and cost; and so interest in this approach has increased rapidly.

There have been a number of attempts to solve the field equations for enclosure fires by numerical methods. These range from laminar models incorporating the Boussinesq approximation and using the stream function–vorticity formulation [3–5], to variable density turbulent models with recirculation using the primitive variable formulation. The ability to deal with the latter resulted largely from the development of the semi-implicit algorithm described by Patankar and Spalding [6]. Recent work includes that of Hasemi [7, 8] and the University of Notre Dame group [9–11].

This paper describes a 2-dim. mathematical model and a new fast solution algorithm for one of the most common problems in fire research, namely the movement of combustion products in a room fire. Combustion is not included, the fire source being

represented in the model by a volumetric mass or heat source, but non-uniform buoyancy forces are allowed to affect both the mean flow and the fluctuating motions. Some validation has been possible by comparing the predictions with data obtained from a series of experiments especially conducted to give predominantly 2-dim. flow.

2. THEORETICAL MODEL

2.1. *The physical problem*

The physical problem concerns a 2-dim., rectangular enclosure with a heat/smoke source, as shown in Fig. 1. For computational purposes the flow domain was extended to the 'free boundary' region outside the doorway.

In this problem the flow is dominated by buoyancy and the turbulence serves to promote the rate of diffusion of mass, momentum and heat (or smoke concentration). In general, cold air is drawn in through the bottom of the opening and passes into the rising plume from a heat (or smoke) source on the floor close to the left-hand wall. A ceiling layer forms comprising heated gases which exit in the upper part of the opening.

2.2. *Nature of the analysis*

The starting point of the present analysis is the set of elliptic partial differential equations that express the conservation of mass, momentum, energy and other fluid variables in steady, 2-dim., recirculating, buoyant flows.

These equations are then reduced to finite domain equations exhibiting 'upwind formulation of the coefficients' over a grid that spans the domain of interest. Suitable hypotheses are made about the physical processes involved. Appropriate initial and boundary conditions are supplied to the procedure which is incorporated into a computer program, MOSIE2 (for Movement of Smoke in Enclosures—2-dim.). Conditions of each test case of interest are supplied to the computer programme and runs made. The primary results of these runs are the grid-node values of the two velocity components, pressure, temperature/smoke concentration, turbulence kinetic energy and eddy dissipation rate. Secondary results like friction factors, heat losses etc. can be derived from the primary results.

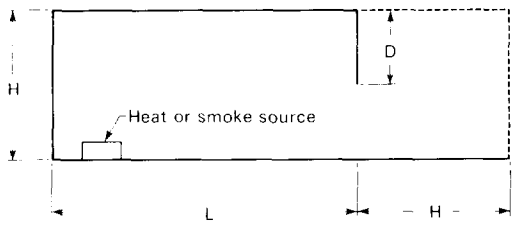

Case (i) H = 2.44m, L = 4.88m, D = 1.22m
(ii) H = 3.0m, L = 9.0m, D = 1.0, 1.5m

FIG. 1. Problem considered; solid lines are solid boundaries, dashed lines are free boundaries.

2.3. *The governing differential equations*

2.3.1. *Variables.* The independent variables of the problem are the two components (x, y) of a Cartesian co-ordinate system. The main dependent variables are the axial and lateral velocity components, u and v, the pressure, p, smoke concentration f or temperature T (or stagnation enthalpy, $\tilde{h}$), the kinetic energy of turbulence, k, and energy dissipation rate, ε.

Apart from the dependent variables, the auxiliary variables that require to be specified by way of algebraic expressions are the density of the air–smoke system, ρ the effective viscosity of the air–smoke system μ_{eff}, and the effective thermal conductivity, λ_{eff} (when solutions to the temperature field are obtained).

2.3.2. *Differential equations.* For steady flow, the time-averaged equations for continuity, velocity components, smoke concentration/temperature, and turbulence variables (where density fluctuation correlations are ignored) take the form:

continuity

$$\frac{\partial(\rho u)}{\partial x} + \frac{\partial(\rho v)}{\partial y} = 0 , \tag{1}$$

x-direction momentum

$$\frac{\partial}{\partial x}(\rho uu) + \frac{\partial}{\partial y}(\rho uv) = \frac{\partial}{\partial x}\left(\mu_{\text{eff}}\frac{\partial u}{\partial x}\right) + \frac{\partial}{\partial y}\left(\mu_{\text{eff}}\frac{\partial u}{\partial y}\right) + S_u , \tag{2}$$

y-direction momentum

$$\frac{\partial}{\partial x}(\rho uv) + \frac{\partial}{\partial y}(\rho vv) = \frac{\partial}{\partial x}\left(\mu_{\text{eff}}\frac{\partial v}{\partial x}\right) + \frac{\partial}{\partial y}\left(\mu_{\text{eff}}\frac{\partial v}{\partial y}\right) + S_v , \tag{3}$$

general transported fluid scalar
(e.g. smoke concentration, temperature)

$$\frac{\partial}{\partial x}(\rho u\phi) + \frac{\partial}{\partial y}(\rho v\phi) = \frac{\partial}{\partial x}\left(\Gamma_{\text{eff},\phi}\frac{\partial \phi}{\partial x}\right) + \frac{\partial}{\partial y}\left(\Gamma_{\text{eff},\phi}\frac{\partial \phi}{\partial y}\right) + S_\phi \tag{4}$$

where S's are appropriate sources and/or sinks of the variables concerned and are given below; μ_{eff} is the effective viscosity described later; and Γ_{eff} is the effective exchange coefficient for the transport of property, ϕ.

The source terms of the above equations are as follows:

$$S_u = \frac{\partial}{\partial x}\left(\mu_{\text{eff}}\frac{\partial u}{\partial x}\right) + \frac{\partial}{\partial y}\left(\mu_{\text{eff}}\frac{\partial v}{\partial x}\right) - \frac{\partial p}{\partial x} , \tag{5}$$

$$S_u = \frac{\partial}{\partial x}\left(\mu_{\text{eff}}\frac{\partial u}{\partial y}\right) + \frac{\partial}{\partial y}\left(\mu_{\text{eff}}\frac{\partial v}{\partial y}\right) - \frac{\partial p}{\partial y} + \rho g\frac{\theta}{T_0}, \quad (6)$$

$$\begin{aligned} S_\phi &= \dot{m}_f''' \quad \text{for} \quad \phi = f, \\ &= \dot{Q}''' \quad \text{for} \quad \phi = \tilde{h} \end{aligned} \quad (7)$$

where $\dot{m}_f'''$, $\dot{Q}'''$ is the strength of the mass/heat source.

2.3.3. *The hydrodynamic turbulence model.* To close this equation set expressions are needed for the local values of μ_{eff} and Γ_{eff}. The two-equation $k \sim \varepsilon$ model of turbulence [12, 13] is used here, as applied for elliptic flows [14, 15]. Since in fire problems buoyancy plays an important role in both promoting (in the rising plume) and inhibiting (in the ceiling layer) turbulent mixing, an extension to the model suggested by Spalding [16] and Rodi [17] has been incorporated.

The $k \sim \varepsilon$ model involves two transport equations for the turbulence characteristics. One of these equations governs the distribution through the field of k, the local kinetic energy of the fluctuating motion; the other governs a turbulence characteristic of different dimensions, namely ε, the energy dissipation rate (first proposed by Harlow and Nakayama [13]). Knowledge of the local values of k and ε allows the evaluation of a local turbulent viscosity, μ_t, from which the turbulent shear stresses are calculated. In the momentum equations the isotropic viscosity μ_t is employed to evaluate the turbulent stresses from their corresponding 'Boussinesq' relations. The combined laminar and turbulent stresses are then expressed by means of μ_{eff}:

$$\mu_{\text{eff}} = \mu_t + \mu, \quad (8)$$

$$\mu_t = \rho C_D k^2/\varepsilon. \quad (9)$$

The effective exchange coefficient for heat $\Gamma_{\text{eff},h}$ is then defined by

$$\Gamma_{\text{eff},h} = \frac{\mu}{\sigma} + \frac{\mu_t}{\sigma_t} \quad (10)$$

where σ, σ_t are the laminar and turbulent Prandtl numbers respectively.

The equations for k and ε are as equation (4) with

$$S_k = G_k + G_B - \rho\varepsilon, \quad (11)$$

$$S_\varepsilon = C_1\frac{\varepsilon}{k}(G_k + G_B)(1 + C_3 R_f) - C_2\frac{\rho\varepsilon^2}{k}. \quad (12)$$

The generation terms are defined as follows:

(i) shear production

$$G_k = \mu_t\left\{2\left[\left(\frac{\partial u}{\partial x}\right)^2 + \left(\frac{\partial v}{\partial y}\right)^2\right] + \left(\frac{\partial u}{\partial y} + \frac{\partial v}{\partial x}\right)^2\right\}, \quad (13)$$

(ii) buoyancy production

$$G_B = -\beta g\frac{\mu_t}{\sigma_{t,\phi}}\frac{\partial\phi}{\partial y} \quad (14)$$

where β is the volumetric expansion coefficient, which for $\phi \equiv T$

$$\beta = -\frac{1}{\rho}\frac{\partial\rho}{\partial T} \quad (15)$$

or for $\phi \equiv f$

$$\beta = -\frac{1}{\rho}\frac{\partial\rho}{\partial f}. \quad (16)$$

The flux Richardson number R_f appearing in S_ε is defined as the ratio of buoyancy to stress production of energy k, i.e.

$$R_f = -G_B/G_k. \quad (17)$$

The above model contains six constants, which were assigned the following values, recommended by Launder and Spalding [18] for free turbulent flows:

$$C_1 = 1.44;\ C_2 = 1.92;\ C_D = 0.09;\ \sigma_k = 1.0;\ \sigma_\varepsilon = 1.3.$$

The above set of constants has been applied successfully to many 2-dim. wall boundary layers [19], duct flows [20], free shear flows [21], recirculating flows [14, 22], and recently also to 3-dim. flows [23, 24]. Complete universality of these constants cannot and should not be expected. It appears, however, from the results presented in Section 4 below, that the same set of constants is also satisfactory for strongly buoyant flows; therefore, the additional complication of replacing constants with functions as suggested, for example, for axisymmetric jets in stagnant surroundings [25] has not been considered further. It is shown below (Section 4.3.) that the effect of buoyancy on the ε-equation is negligible, and therefore, C_1 and C_2 (which appear only in that equation) should retain the values found appropriate for non-buoyant flows. Some fine tuning of the remaining three constants, by computer optimisation, will be considered in future work. The sixth constant C_3 controlling the effect of buoyancy on the ε-equation is discussed below.

In the above equations, G_B represents an exchange between the turbulent kinetic energy k, and the potential energy. In stable stratification G_B becomes a sink term so that the turbulent mixing is reduced while the potential energy increases. In unstable stratification the buoyancy will enhance turbulence since G_B is positive.

For the definition of flux Richardson number given by equation (17), C_3 should be close to zero for vertical shear layers and close to unity for horizontal shear layers.

Rodi [7], has suggested an alternative definition of the flux Richardson number which enables a single value of $C_3 \simeq 0.8$ to be used in both vertical and horizontal layers. The alternative definition of R_f is

$$R_f = -\frac{G_{BL}}{2(G_k + G_B)} \quad (18)$$

where G_{BL} is the buoyancy production of the lateral energy component.

In *horizontal shear layers* where the lateral velocity component is in the direction of gravity, all buoyancy production is in this direction so that

$$G_{BL} = 2G_B \tag{19}$$

and

$$R_f = -\frac{G_B}{(G_k + G_B)}. \tag{20}$$

In *vertical layers* the lateral component is normal to the direction of gravity and receives no buoyancy contribution so that

$$G_{BL} = 0\,, \tag{21}$$

and therefore

$$R_f = 0. \tag{22}$$

The latter approach was adopted for this study.

3. METHOD OF SOLUTION

3.1. *The finite-domain equations*

The finite-difference technique used combines features of the SIMPLE and NEAT algorithms (Patankar and Spalding [6], and Spalding [26]) together with a new whole-field pressure-correction algorithm.

The solution domain is subdivided by a rectangular finite-difference grid (Fig. 2).

Algebraic equations of the form

$$(\Sigma A_i - S_p)\,\phi_p = \Sigma(A_i\phi_i) + S_u \tag{23}$$

relate nodal values of each variable ϕ at node P to values at the four neighbouring nodes, i, and are derived by integration of the differential equations given in the previous section over an elementary control volume or cell surrounding the node. The summation is over the four N,S,E,W adjacent cells, the coefficient A_i contains convective and diffusive links between cell P and cell i and $(S_u + S_P\,\phi_P)$ is the source term integrated over the cell.

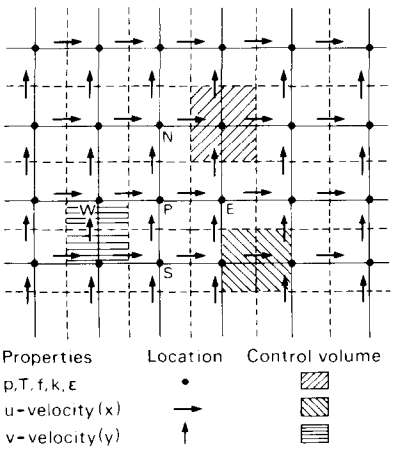

FIG. 2. Finite-difference grid and control volumes.

Two features of the integration should be mentioned. Firstly in the convective term upwind-differencing is used (i.e. the value of ϕ crossing the cell face is taken to be that at the node on the upwind side); secondly, the integrated source term is expressed in linear form $(S_u + S_P\,\phi_P)$. Both these practices are widely used to enhance numerical stability.

3.2. *The pressure field*

Pressures are obtained from a pressure correction equation which yields the pressure change needed to procure velocity and density changes to satisfy mass continuity. The pressure correction equation has the form

$$\Sigma A_i p'_P = \Sigma(A_i p_i) - m_P \tag{24}$$

where m_P is the mass continuity error for cell P and p'_P is the pressure correction made to satisfy continuity for cell P.

The pressure correction equation is solved two-dimensionally, as follows: equation (24) is written as

$$A_P p'_{i,j} = A_N p'_{i,j+1} + A_S p'_{i,j-1} + A_E p'_{i+1,j} + A_w p'_{i-1,j} + b. \tag{25}$$

Suppose

$$p'_{i,j} = N_{i,j}\,p'_{i,j+1} + E_{i,j}\,p'_{i+1,j} + B_{i,j} \tag{26}$$

then

$$p'_{i,j-1} = N_{i,j-1}\,p'_{i,j} + E_{i,j-1} + p'_{i+1,j-1} + B_{i,j-1}. \tag{27}$$

$$p'_{i-1,j} = N_{i-1,j}\,p'_{i-1,j+1} + E_{i-1,j}\,p'_{i,j} + B_{i-1,j}. \tag{28}$$

Substitution yields

$$p'_{i,j}(A_P - A_S N_{i,j-1} - A_w E_{i-1,j}) = A_N p'_{i,j+1} + A_E p'_{i+1,j} + b + A_S(E_{i,j-1}p'_{i+1,j-1} + B_{i,j-1}) + A_w(N_{i-1,j}\,p'_{i-1,j+1} + B_{i-1,j}) \tag{29}$$

hence

$$N_{i,j} \equiv A_N/D_{i,j},$$

$$E_{i,j} \equiv A_E/D_{i,j},$$

$$B_{i,j} \equiv [b + A_S(E_{i,j-1}\,p'_{i+1,j-1} + B_{i,j-1}) + A_w(N_{i-1,j}\,p'_{i-1,j+1} + B_{i-1,j})]/D_{i,j}$$

where

$$D_{i,j} \equiv A_P - A_S N_{i,j-1} - A_w E_{i-1,j}.$$

Therefore the pressure field is obtained as follows:

(i) compute $N_{i,j}$, $E_{i,j}$, $D_{i,j}$ starting at low i, j and store two-dimensionally;
(ii) compute $B_{i,j}$ repeatedly using the in-store $p'_{i+1,j-1}$, $p'_{i-1,j+1}$;
(iii) compute $p'_{i,j}$ starting at high i, j;
(iv) repeat until convergence.

3.3. *Solution sequence*

Solution is obtained by sweeping through the

calculation domain, solving successively at each constant x-line (see Fig. 2) and proceeding from inlet to outlet, only one traverse being made at each line before moving downstream. The solution sequence is thus, as follows:

(a) Conservation equations are solved at each x-constant line for u, v, k, ε, h, using the Jacobi method for u and v, and the tri-diagonal matrix algorithm (TDMA) for the other variables. An assumed pressure distribution is used to solve these equations.

(b) T, ρ, μ_t are updated. T is derived from h, u, v, k. The density is calculated from the gas law with the assumed pressure.

Steps (a) and (b) are repeated line-by-line to the completion of a sweep.

(c) When the whole field is swept, as above, the pressure correction equation is solved using the mass errors that have been calculated during the sweep, and u and v are updated accordingly.

(d) Control is returned to (a) and a new sweep starts; the sequence is repeated until convergence is attained.

3.4. *Boundary and initial conditions*

3.4.1. *Boundary conditions.* For this problem there are two types of boundary: solid or free. On a solid boundary the no-slip condition on the velocity components is employed. If smoke concentration is a dependent variable, an adiabatic wall condition is used. For the temperature equation, adiabatic side walls and either adiabatic floor and ceiling or finite floor and ceiling heat fluxes were considered. The fluxes of momentum and heat to the wall obey the wall-function relations of Launder and Spalding [12].

For the kinetic energy of turbulence, the zero diffusive flux at the wall is used. For the dissipation rate, the empirical evidence that a typical length scale of turbulence varies linearly with the distance from the wall, is used to calculate ε itself at the near-wall point.

It is realised that with temperature stratification the equivalent of the "law of the wall" is the Monin–Obukov log-linear profile [27]. However at present the conventional logarithmic law is employed. The Monin–Obukov law is under study.

On the free boundaries the pressure is prescribed. The derivative of the velocity components normal to the free surfaces are equated to zero. The smoke concentration or temperature conditions at the vertical, right-hand free boundary are prescribed as follows: at points of in-flow, ambient temperature or zero concentration is specified, at points of outflow the derivative of the dependent variable is equated to zero.

3.4.2. *Initial conditions.* In many cases, computations are started with the solution of a previous run as an initial condition. However, when making the first calculation initial velocity fields are deduced from a stream function guess. The air flow rate is estimated by equating the rate of work done by the gravity force on the fluid to the net rate of input of kinetic energy to the system. The enclosure is divided into three regions and the circulation is then superimposed on the air flow rate in each region to give the initial guess of the stream function.

A more sophisticated procedure is the solution of the stream function equation with a prescribed vorticity source; the latter is deduced from a prescribed velocity profile at the opening. This procedure has been developed but has not been used for the results presented here.

The temperature or smoke concentration is set initially by assuming a vertical linear relationship between height and T or f ranging from 750 K to ambient or 1.0 to zero respectively. A uniform pressure field is also used as an initial condition.

3.5. *Computational details*

Most work has been conducted with a 42 × 22 grid in order to compare results with the Notre Dame study [9–11]. The grid spacing was non-uniform with grid lines more closely spaced near the walls. The horizontal spacing outside the compartment was also coarser being twice that at the source plume. Between 500 and 1000 sweeps of the whole field were necessary in order to obtain convergence. Two computers have been used at various times during this study, an ICL1904S 'mainframe' and a PRIME 550 'minicomputer' which have broadly similar speeds. Execution times per 1000 sweeps from the initial conditions range from around 220 min for solving the full $k \sim \varepsilon$ model to around 140 min for a fixed viscosity problem. A few trials have been conducted on a CRAY 1 'Supercomputer'. Execution times reduce dramatically to around 110 s without any changes to the existing code. Extra improvement should be possible by suitable modifications to aid in vectorization of the code.

Results were reasonably insensitive to grid size. Several runs were performed with a 16 × 11 grid which produced predictions very close to those from the 42 × 22 grid in flows where there was no small scale structure. Obviously the coarser grid could not be expected to, and did not, predict the multi-layering phenomenon (see below).

4. RESULTS AND VALIDATION

The validation of a 2-dim. code predicting convection transfer presents some problems. Although there are considerable experimental data available from full-scale fire experiments these are not particularly suitable because they all have a strong transverse element in their flows.

Comparisons have therefore been made with the predictions of the Notre Dame 2-dim. code as well as with experimental data obtained in some specially conducted full-scale experiments designed to give nearly 2-dim. flow behaviour. The gross differences between the two computer programs are in their treatment of time, unsteady in the Notre Dame study, and of turbulence, mixing length and algebraic models having been used in that work. Both however employ

aspects of the SIMPLE algorithm.

Neither validation was entirely satisfactory since the experimental data were not as thorough as is desirable and, of course, the comparison with the Notre Dame code is somewhat circular. However, the particular aspect of the Notre Dame predictions, that in certain circumstances not two but four layers of gas movement can be detected in a corridor fire was an interesting test supported, qualitatively at least, by experimental observation [28].

4.1. *Comparisons with the Notre Dame results*

The identical problem to that studied by the Notre Dame group was examined using MOSIE2, see Fig. 1. An enclosure with $H = 2.44$ m, $L = 4.88$ m, $D = 1.22$ m contains a volumetric heat source of 527 kW power distributed over a depth H normal to the plane of calculation. This source is situated on the floor of the compartment centred 0.8 m from the closed wall. The end walls provide adiabatic boundary conditions with the floor and ceiling presenting finite heat conductances.

The fields of horizontal velocity component, u, and the temperature, T, at $x = L/2$ and L are illustrated in Fig. 3 for both programs where a fixed effective viscosity of 20 μ has been assumed.

The results from MOSIE2 are, of course, for steady state conditions and for the Notre Dame code are for a real elapsed fire time of 30 s. The agreement between the two codes is quite good, both revealing the four-layer structure in the u field. A velocity vector plot from MOSIE2 is presented in Fig. 4 illustrating the largely stagnant area at the centre of the enclosure where the flow reversal is occurring. The use of this viscosity field is artificial because although it predicts similar qualitative behaviour to the experiments of McCaffrey and Quintiere [28] there is little alternative justification for its use.

The effect of different viscosity models at $x = L/2$ on the u and T field is shown in Fig. 5. Using fixed viscosity models the multilayering disappears between 200 and 400 μ. The $k \sim \varepsilon$ model (with $C_3 = 0.9$—the effect of varying C_3 is discussed below) produces no multilayering. Indeed, the $k \sim \varepsilon$ model predicts effective viscosities around 2000 μ in the upper regions of the room, much higher than the upper limit of 400 μ imposed by the Notre Dame programme.

The four-layer structure observed in the experiments of McCaffrey and Quintiere is not clearly understood. The capacity of these 2-dim. codes to predict such a flow in certain, low turbulence conditions may be misleading since the experiment had a substantial three-dimensional flow character not modelled here. However, it has allowed a comparison between the codes and will be pursued further with the 3-dim. version of this program.

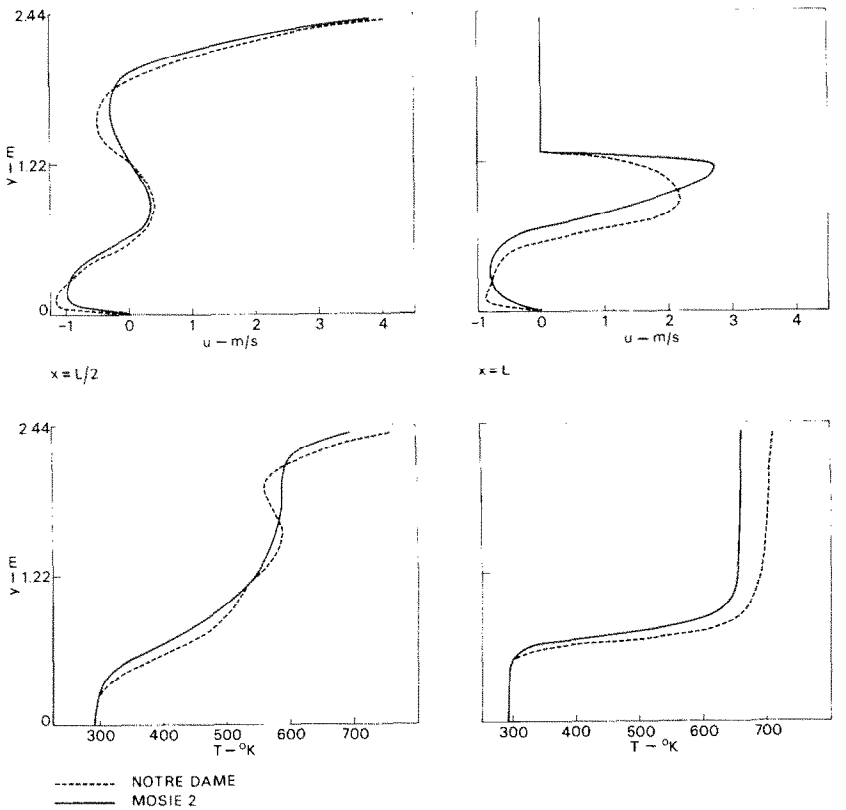

FIG. 3. Horizontal velocity component u and temperature T fields at $x = L/2$ and L for $\mu_{\text{eff}} = 20$.

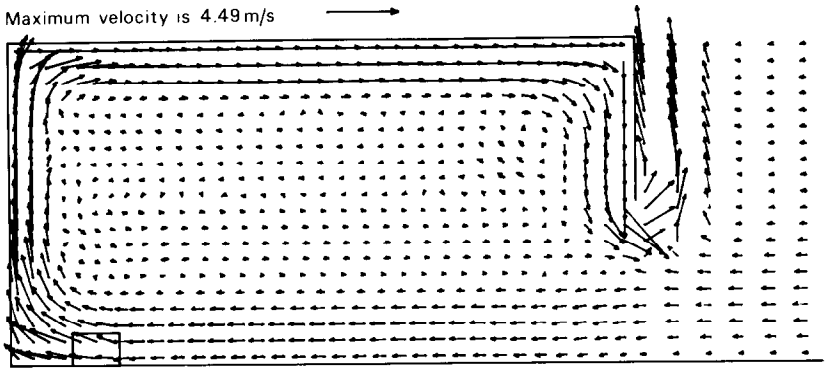

FIG. 4. Velocity vectors from MOSIE2 for $\mu_{eff} = 20$.

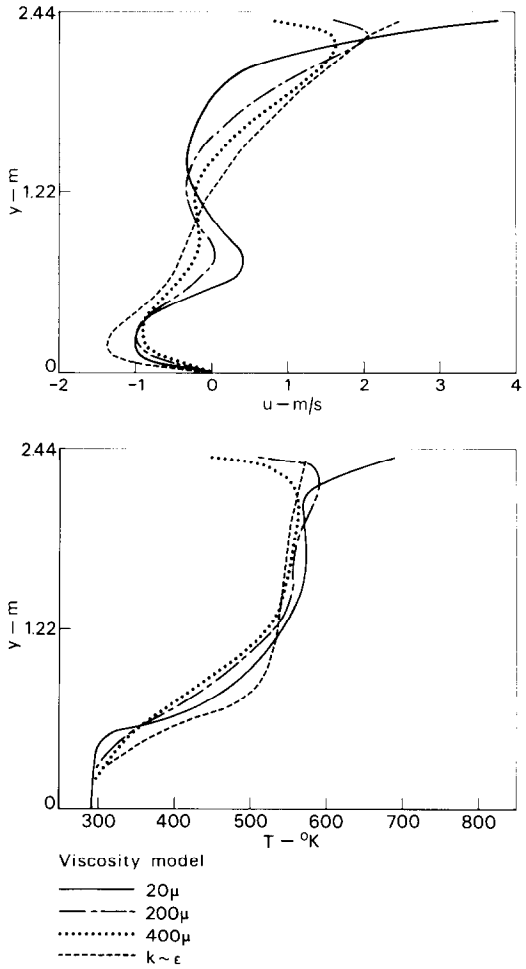

FIG. 5. Effect of turbulent viscosity and u and T fields at $x = L/2$.

4.2. *Experimental work*

A short series of experiments were conducted in the mall of a shopping-mall test facility at the Fire Research Station just prior to demolition. This building, described in detail by Heselden [29], was of a construction to withstand repeated fire experiments within the shops but the mall itself was not so protected. Only four experiments were possible before the fabric of the mall allowed excessive air leakages into the system which are not accounted for by the programme.

The resulting compartment was 3 m high by 9 m long with adjustable soffit depth between 1 and 1.5 m. The compartment was 6 m wide and a strip fire source of 3 rectangular pans 0.5 × 2 m were laid across the mall 1.25 m from the rear wall. The fuel was industrial methylated spirit and the heat output was calculated from the weight loss of the central pan as 2.04 MW. This heat output was maintained for a period of about 10 min during which time approximately steady conditions prevailed. The flame length extended to approximately half the compartment height.

The vertical temperature profile on the centreline of the compartment was monitored at three locations by columns of nine thermocouples each 0.3 m apart in the y direction. The columns were situated at I, J, K, see Fig. 6, 2.56 m, 5.76 and 8.96 m from the rear wall ($x = 0$). The output of each thermocouple was sampled at 15 s intervals. The horizontal velocity profile was monitored at only one location (Column J) by a column of 8 water-cooled vane anemometers [30] each 0.4 m apart in the y direction at $x = 5.46$ m. The velocities at each anemometer were sampled at 60 s intervals. A smoke rake was also placed close to the anemometer column to visualise the flow and indicate any multi-layering not detected by the anemometers. Figure 6 shows a plan view of the mall with instrumentation and modifications incorporated for this work.

4.3. *Comparisons with experimental data*

The heat input used for the program was 270 kW/m being the product of the measured rate of mass loss of the fuel and the net calorific value less 20% for

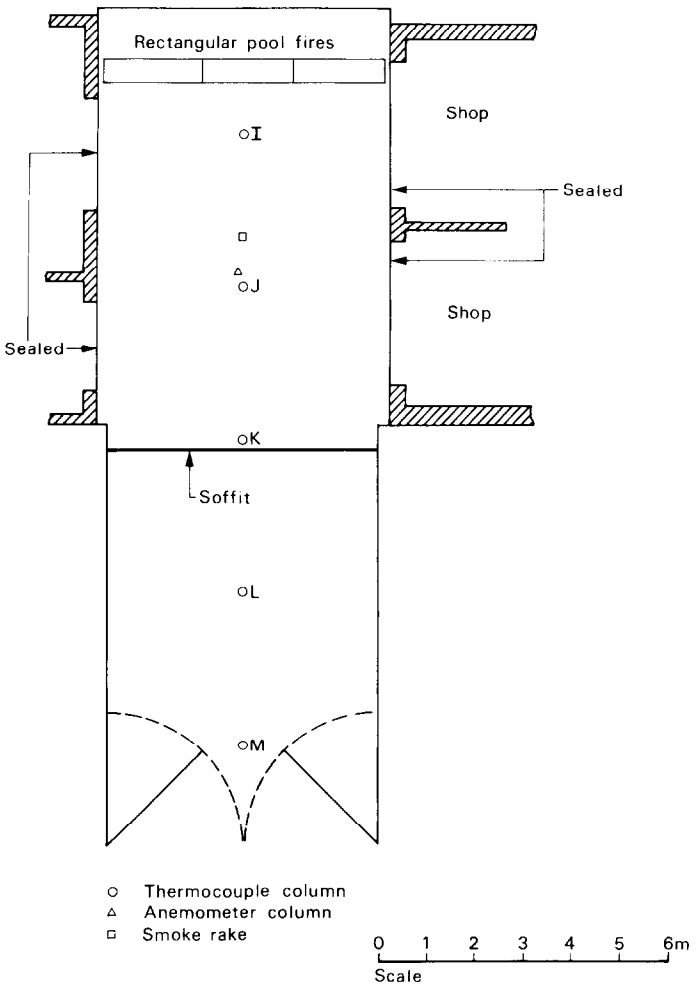

FIG. 6. Plan of mall showing instrumentation.

radiation energy loss. The heat source was uniformly distributed over two cells in the x co-ordinate (0.45 m) and 13 cells (1.73 m) in the y co-ordinate to approximately simulate the release of heat over the whole flame length.

An ambient temperature of 293 K was assumed with isothermal ceiling and floor boundary conditions. Two geometrical configurations were studied with soffit depth, D, 1 m and 1.5 m. Predictions of the fields of velocity, u, and temperature T, using the $k \sim \varepsilon$ model are illustrated in Figs. 7 and 8 together with experimental data where possible. Comparisons are with predicted values at all nodes closest to the measurement stations.

Velocity vectors for the two situations are shown in Fig. 9. No attempt has been made to optimise the constants in the model by comparisons with the data. The constant C_3 was taken as 0.9 in the above work. The prediction of a deep layer of hot gases with roughly uniform temperature bounded at the lower edge by a steep gradient to ambient temperature is particularly gratifying.

The detailed agreement with experimental data, as shown in Figs. 7 and 8, is reasonable with a tendency to under-predict mean temperature in the hot gas layer particularly close to the source. The experimental temperature data close to the source will be subject to a radiation error apparently about 50°C at the bottom of Column I. There is also a tendency to over-predict the depth of the hot layer particularly noticeable at the opening. The predictions of u velocity are not unreasonable when it is realised that the anemometers will not turn until experiencing a velocity in excess of 0.5 m/s. There is some evidence that the detailed velocity gradient at the ceiling is not being accurately represented although better experimental data are needed to confirm this. No four-layer structure was observed in the experiment and could not be predicted even by introducing a fixed effective viscosity of 20 μ unless the heat source was restricted in height. Running with adiabatic boundary conditions at both vertical and horizontal boundaries produced only small differences.

A parametric study of C_3 was undertaken since this appears to have the least evidence to support any particular value. Some results are presented in Fig. 10 at $x = L/2$. There was no significant difference in the predictions with C_3 in the range 1.0 (no buoyancy contribution in the ε equation) to 0.3. Below 0.3 some problems of convergence were experienced. However with $C_3 = 1.0$ and $G_B = 0$ in the k equation, no buoyancy effects in either equation, a significant change, occurred. The stratified layer disappeared, and was replaced by a more homogeneous flow with maximum predicted temperatures much higher than before, indicating that in this case the compartment acts as a 'recuperator'.

5. DISCUSSION AND CONCLUSIONS

It has not been the intention of this study to investigate the effect of the controlling non-

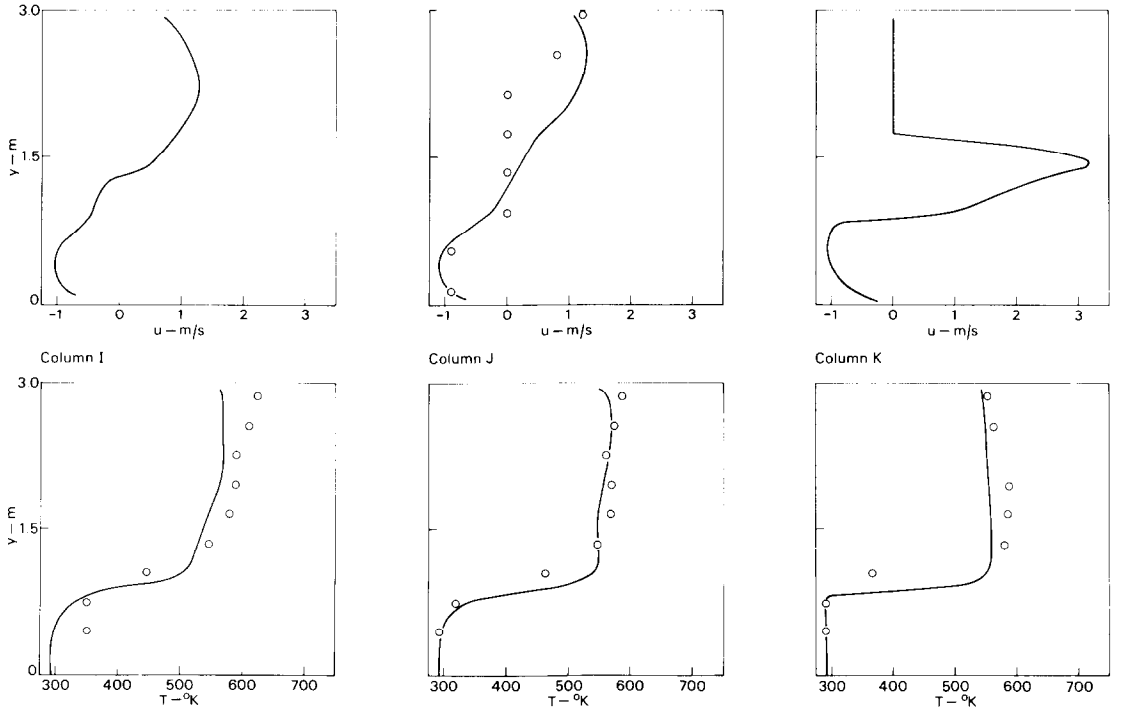

Fig. 7. Predicted and measured velocity and temperature profiles for $D = 1.5$ m.

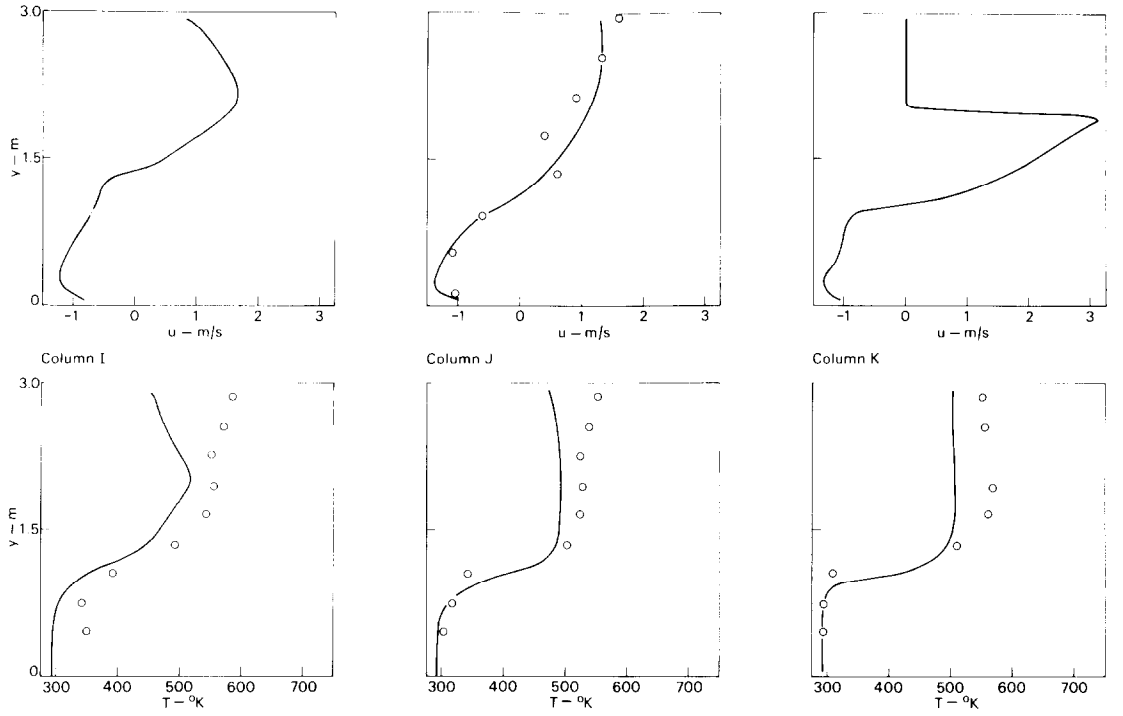

FIG. 8. Predicted and measured velocity and temperature profiles for $D = 1$ m.

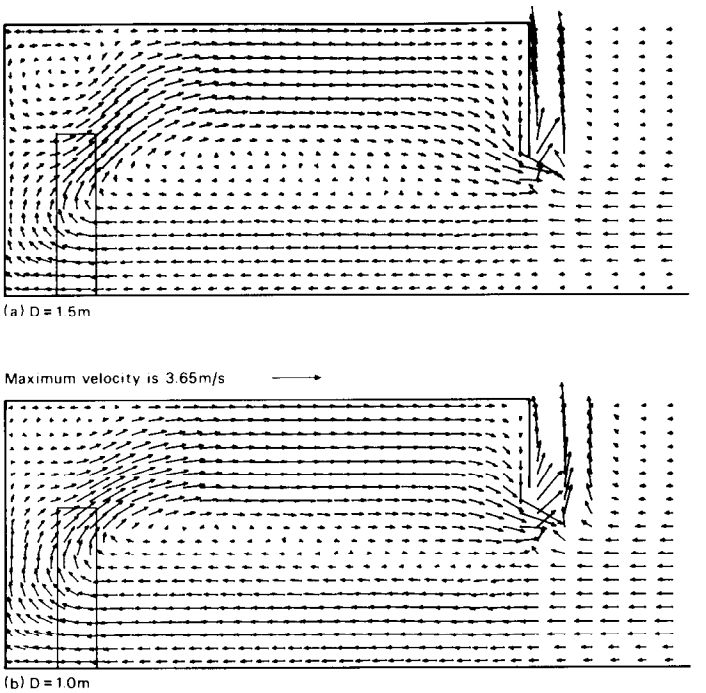

FIG. 9. Velocity vectors for experimental conditions.

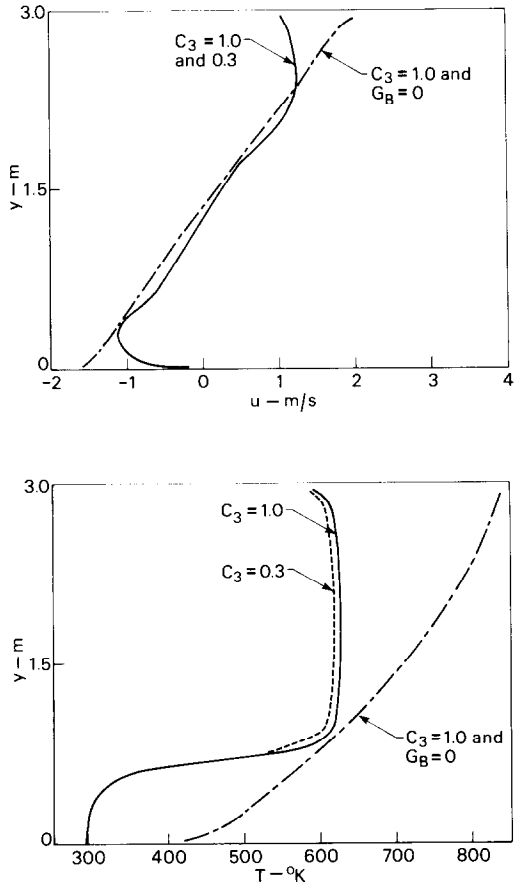

FIG. 10. Effect of C_3 on predictions of u and T at $x = L/2$.

dimensional variable, the Grashof number, because of lack of validating data. Indeed, in practical cases, the definition used by other workers becomes ambiguous with a distributed heat source. All the work was conducted with Grashof number in the region of 10^{12}, based on model height.

Although the code could have been used in its time-dependent mode, only the more difficult case of establishing a genuine steady-state was attempted. The reason for using this approach was that for one of the applications envisaged, namely aiding the design of smoke control devices (e.g. natural or forced ventilation of smoke) the worst case must be accounted for, i.e. the maximum volume of smoke from a steady-state fire at flashover. Nearly all experimental test and model work with which this model is being validated are conducted in this way.

The above results have demonstrated the capabilities of the present prediction technique in modelling turbulent smoke movement in 2-dim. enclosures. It is encouraging to see that the computed results indicate the correct trends, and that the buoyancy modifications to the turbulence model do improve the realism of the predictions. Where comparisons with experimental data have been possible the predictions give reasonable agreement with those data. Some uncertainty remains over the turbulence model constants employed, particularly C_D, but clearly the effect of introducing a buoyancy term into the k equation was far more important than the precise value of the constant C_3 in the ε-equation. Indeed, there is evidence, although not conclusive, that it is only the k equation that should reflect the effects of buoyancy.

Real fires appear to have a significant large scale periodic behaviour impressed upon their turbulence spectrum. Although apparently 'adequate' the $k \sim \varepsilon$ model may, therefore, not be the best choice and other models as, for example, the one suggested by Hanjalic and Launder [31] which attempts to account for differences in the spectrum shape may provide some lead in this direction.

It is evident, however, that to validate thoroughly such a mathematical model either better experimental data with 2-dim. features should be obtained or that a 3-dim. version of the model should be employed where more data are available. Clearly the latter is more desirable since it is for 3-dim. problems that the code would eventually be used. Development of such a code is under way and will be the subject of future work.

Acknowledgements—The authors wish to acknowledge the help of R. Chitty and H. Wraight with the experimental work and to thank Professor K. T. Yang of University of Notre Dame for the use of the UNDSAFE I code.

This paper forms part of the work of the Fire Research Station, Building Research Establishment, Department of the Environment, U.K. It is contributed by permission of the Director, Building Research Establishment.

REFERENCES

1. F. A. Williams, Scaling mass fires, *Fire Res. Abs. Revs.* **11**, 1 (1969).
2. D. B. Spalding, *Ninth Symposium (International) on Combustion* p. 833. Academic Press (1963).
3. K. E. Torrance and J. A. Rockett, Numerical study of natural convection in an enclosure with localised heating from below—Creeping flow to the onset of laminar instability, *J. Fluid Mech.* **36**, 33 (1969).
4. D. W. Larson and R. Viskanta, Transient combined laminar free convection and radiation in a rectangular enclosure, *J. Fluid Mech.* **78**, 65 (1976).
5. C. Knight, Numerical studies of natural convection in an enclosure, Harvard University Division of Engineering and Applied Physics, Technical Report 15 (1976).
6. S. V. Patankar and D. B. Spalding, A calculation procedure for heat, mass and momentum transfer in three-dimensional parabolic flows, *Int. J. Heat Mass Transfer* **15**, 1787 (1972).
7. Y. Hasemi, Numerical simulation of fire phenomena and its application, Building Research Institute of Japan, Paper 66 (1976).
8. Y. Hasemi, Numerical calculation of the natural convection in fire compartment. BRL Res. Paper No. 69, Building Res. Inst. Min. of Const. Japan, Feb 1977.
9. A. C. Ku, M. L. Doria and J. R. Lloyd, *16th Symposium (International) on Combustion* p. 1373. The Combustion Institute (1977).
10. K. T. Yang and J. C. Chang, UNDSAFE-I. A computer code for buoyant flow in an enclosure. University of Notre Dame Technical Report TR 79002-77-1 (1977).

11. V. K. Liu and K. T. Yang, UNDSAFE-II. A computer code for buoyant turbulent flow in an enclosure with thermal radiation. University of Notre Dame Technical Report TR-79002-78-3 (1978).
12. B. E. Launder and D. B. Spalding, *Mathematical Models of Turbulence*. Academic Press, London (1972).
13. F. H. Harlow and P. I. Nakayama, Transport of turbulence energy decay rate. Los Alamos Sci. Lab., Univ. Calif. REP LA-3854 (1968).
14. N. C. Markatos, Transient flow and heat transfer of liquid sodium coolant in the outlet plenum of a fast nuclear reactor, *Int. J. Heat Mass Transfer* **21**, 1565 (1978).
15. N. C. Markatos and A. Moult, The computation of steady and unsteady turbulent, chemically reacting flows in axi-symmetrical domains, *Trans Inst. chem. Engrs* **57**, 156 (1979).
16. D. B. Spalding, Turbulence Models. Imperial College Mechanical Engineering Dept. Report HTS/76/17 (1976).
17. W. Rodi, Turbulence Models and their Application in Hydraulics—A State of the Art Review. University of Karlsruhe SFB 80/T/127 (1978).
18. B. E. Launder and D. B. Spalding, The numerical computation of turbulent flows, *Comp. Methods. appl. Mech. Engng* **3**, 269 (1974).
19. W. P. Jones and B. E. Launder, The prediction of laminarization with a two-equation model of turbulence, *Int. J. Heat Mass Transfer* **15**, 301 (1972).
20. P. L. Stephenson, Theoretical study of heat transfer in two-dimensional turbulent flow in a circular pipe and between parallel and diverging plates, *Int. J. Heat Mass Transfer* **19**, 413 (1976).
21. B. E. Launder, A. P. Morse, W. Rodi and D. B. Spalding, The prediction of free-shear flows—a comparison of the performance of six turbulence models, *Proc. NASA Langley Free Turbulent Shear Flows Conf.*, Vol. 1, NASA SP320 (1973).
22. A. K. Rastogi and W. Rodi, Predictions of heat and mass transfer in open channels, *J. Hydraulics Div., ASCE* No. HY3, pp. 397–420 (1978).
23. J. J. McGuirk and W. Rodi, The Calculation of Three-Dimensional Turbulent Free Jets, *Turbulent Shear Flows 1*, Springer, Heidelberg (1979).
24. N. C. Markatos, M. R. Malin and D. G. Tatchell, Computer analysis of three-dimensional turbulent flows around ships' hulls, *Proc. Inst. mech. Engrs* **194**(24), 239 (1980).
25. W. Rodi, The prediction of free turbulent boundary layers by use of a two-equation model of turbulence. PhD Thesis, Univ. of London (1972).
26. D. B. Spalding, The calculation of free convection phenomena in gas–liquid mixtures, in *Heat Transfer and Turbulent Buoyant Convection* (Edited by D. B. Spalding and N. Afgan) p. 569. Hemisphere, Washington (1977).
27. A. S. Monin and A. M. Obukov, Basic laws of turbulent mixing in the ground layer of the atmosphere, *Trudy, Geofiz. Inst. An-SSR* **151**(24) 163–187 (1954).
28. B. J. McCaffrey and J. G. Quintiere, Buoyancy driven countercurrent flows by a fire source, in *Heat Transfer and Turbulent Buoyant Convection* (Edited by D. B. Spalding and N. Afgan) p. 457, Hemisphere, Washington (1977).
29. A. J. M. Heselden, Fire problems of pedestrian precincts. Part 1. The smoke production of various materials. Joint Fire Research Organisation, Fire Research Station. Fire Research Note 856 (1971).
30. T. Y. Palmer and L. E. Northcutt, A high temperature water-cooled anemometer. *Fire Technol.* **7**, 201 (1971).
31. K. Hanjalic and B. E. Launder, Turbulent transport modelling of separating and reattaching shear flows. University of California Davis Report TF/78/8 (1978).

MODELE MATHEMATIQUE D'UN ECOULEMENT DE FUMEE INDUIT NATURELLEMENT DANS DES CAVITES

Résumé—On reporte une méthode de calcul des distributions de vitesse et de température dans des cavités contenant une source de feu. La procédure est basée sur la solution, aux différences finies, des équations bidimensionnelles de conservation de la masse, de la quantité de mouvement, de l'énergie, de l'énergie de turbulence et du taux de dissipation de turbulence, avec des relations de fermeture pour la viscosité et la diffusivité thermique par turbulence. On inclut la convection naturelle dans ce modèle turbulent. Les résultats sont en accord raisonnable avec les données expérimentales.

MATHEMATISCHE MODELLBILDUNG DER DURCH AUFTRIEBSKRÄFTE HERVORGERUFENEN RAUCHSTRÖMUNG IN GESCHLOSSENEN RÄUMEN

Zusammenfassung—Es wird ein numerisches Verfahren zur Berechnung von Geschwindigkeits- und Temperaturverteilungen in geschlossenen Räumen beschrieben, die einen Brandherd enthalten. Das Verfahren basiert auf der Lösung (nach einem endlichen Differenzenverfahren) der zweidimensionalen Gleichungen für die Erhaltung der Masse, des Impulses, der Energie, der Turbulenzenergie und des Wirbeldissipations verhältnisses, mit geschlossenen Ausdrücken für die turbulente Zähigkeit und Temperaturleitfähigkeit. Die Einflüsse des Auftriebs auf das Turbulenzmodell wurden mit einbezogen. Die Ergebnisse befinden sich in angemessener Übereinstimmung mit den experimentellen Werten.

МАТЕМАТИЧЕСКОЕ МОДЕЛИРОВАНИЕ ТЕЧЕНИЯ ДЫМА В ЗАМКНУТЫХ ОБЪЕМАХ ПОД ВОЗДЕЙСТВИЕМ ПОДЪЕМНОЙ СИЛЫ

Аннотация — Предложен численный метод расчета распределения скорости и температуры в объемах, содержащих источник пламени. Метод основан на конечно-разностном решении двухмерных уравнений сохранения массы, движения, энергии, энергии турбулентности и скорости диссипации вихрей, с замыкающими уравнениями для турбулентной вязкости в температуропроводности. В модели турбулентности учитывается влияние подъемной силы. Показано, что полученные результаты находятся в удовлетворительном согласии с экспериментальными данными.